

**LATERAL FLOW NITROCELLULOSE MEMBRANE FOR DIAGNOSTIC
KIT APPLICATION: SYNTHESIS, CHARACTERIZATION AND
PERFORMANCE EVALUATION**

LOW SIEW CHUN

UNIVERSITI SAINS MALAYSIA

2010

**LATERAL FLOW NITROCELLULOSE MEMBRANE FOR DIAGNOSTIC
KIT APPLICATION: SYNTHESIS, CHARACTERIZATION AND
PERFORMANCE EVALUATION**

by

LOW SIEW CHUN

**Thesis submitted in fulfillment of the requirements
for the degree of
Doctor of Philosophy**

APRIL 2010

ACKNOWLEDGEMENTS

First of all, I would like to express my deepest gratitude to my parents Mr. Low Heng Kui and Madam Yeo Siok Hong for their endless love and blessing for me to pursue my PhD degree. Thank you for your persevering support and encouragement.

My deepest appreciation also goes to my main supervisor, Prof. Abdul Latif Ahmad, and both of my co-supervisors, Dr. Syamsul Rizal Abd Shukor and Y. Brs. Prof. Asma Ismail for their prestigious guidance and supervision, constant attention, valuable suggestions and enthusiastic supports throughout the course of my research.

I would also like to express my heart-felt gratitude to all lecturers in the School of Chemical Engineering USM for giving me support and guidance, especially to Assoc. Prof. Dr. W James Noel Fernando and Dr. Ooi Boon Seng, who have shared their precious knowledge of mathematic modelling and membrane technology with me. I extend my gratitude to all the laboratory technicians and administrative staff of the School of Chemical Engineering and the Institute for Molecular Medicine Research (INFORMM) for the assistance rendered to me.

On top of that, special thanks to Dr. Hans Beer, Dr. Jan Gutenwik, Amy Amilda Anthony, Pei Ching, Lian See, Ee Mee and Siang Piao for the unending help throughout the research. To Jia Huey, Choi Yee, Choe Peng, Derek, Sumathi, Ramesh, Hairul, Sunarti, Lip Han, Sam, Yin Fong, Kelly, Thiam Leng, Mei Fong, Lau, Ivy, Foo and others whom I am not able to address here; thank you for your

support as well as making my life interesting and cheerful. I would also like to express my appreciation to my sisters, Siew Luan and Siew Yi, my brothers, Hock Foo and Hock Jeng, my brother-in-law, Brandon Tai and finally to the one special to my heart, Alan Lim for giving me perpetual supports, riding along with me for the ups and downs of my life as well as giving me endless patience all this while.

Last but not least, I wish to show my grateful thanks to the Ministry of Education and Universiti Sains Malaysia for providing me the financial support under ScienceFund (Project: A/C No: 6013326) and to the Malaysian Technology Development Corporation for granting the Commercialisation of R&D Fund (CRDF) (Project A/C No: 6053014). I would also like to express my acknowledgement to Universiti Sains Malaysia for providing me the postgraduate scholarship - Fellowship. To all the people who have helped me throughout my research, directly or indirectly; your contribution will be remembered ceaselessly. Thank you.

Low Siew Chun
April 2010

TABLE OF CONTENTS

| | Page |
|--|-------|
| ACKNOWLEDGEMENTS | ii |
| TABLE OF CONTENTS | iv |
| LIST OF TABLES | x |
| LIST OF FIGURES | xiii |
| LIST OF PLATES | xviii |
| LIST OF ABBREVIATIONS | xx |
| LIST OF SYMBOLS | xxii |
| ABSTRAK | xxv |
| ABSTRACT | xxvii |
| | |
| CHAPTER 1 – INTRODUCTION | |
| | |
| 1.1 Membrane overview | 1 |
| 1.2 Lateral flow nitrocellulose (NC) membrane | 3 |
| 1.3 Lateral flow NC membrane for biomedical application | 4 |
| 1.4 Diagnostic kit | 5 |
| 1.5 Problem statement | 7 |
| 1.6 Research objectives | 9 |
| 1.7 Scope of study | 10 |
| 1.8 Organization of the thesis | 13 |
| | |
| CHAPTER 2 – LITERATURE REVIEW | |
| | |
| 2.1 Membrane classification | 15 |
| 2.2 Chronological development of nitrocellulose membrane | 18 |
| 2.3 Properties of NC membrane | 19 |
| 2.3.1 Chemical and physical properties of NC polymer | 20 |
| 2.3.2 Structural and characterization of NC membrane | 21 |
| 2.4 Potential application of NC membrane in immunoassay | 23 |
| 2.5 Development of NC membrane | 24 |

| | | |
|-----------|---|----|
| 2.5.1 | Membrane fabrication technique: phase inversion | 25 |
| 2.5.2 | Membrane formulation | 30 |
| 2.5.2 (a) | Polymer | 31 |
| 2.5.2 (b) | Solvent | 31 |
| 2.5.2 (c) | Non-solvent or pore former | 32 |
| 2.5.2 (d) | Additive and wetting agent | 33 |
| 2.5.3 | Effects of preparation condition | 34 |
| 2.5.3 (a) | Membrane casting thickness | 35 |
| 2.5.3 (b) | Relative humidity | 36 |
| 2.5.3 (c) | Solvent evaporation time and temperature | 36 |
| 2.6 | Modification of membrane morphology | 37 |
| 2.6.1 | Common membrane modification methods | 38 |
| 2.6.2 | Thermal-mechanical stretching techniques | 41 |
| 2.7 | Statistical analysis on membrane fabrication and modification | 45 |
| 2.7.1 | Cross-Mixture-Process design | 45 |
| 2.7.2 | Response Surface Methodology (RSM) | 47 |
| 2.8 | Immunochromatography testing | 48 |
| 2.8.1 | Working mechanism of immunochromatography testing | 49 |
| 2.8.2 | Protein immobilization | 52 |
| 2.8.3 | Effects of working conditions on immunodiagnostic testing | 54 |

CHAPTER 3 – TRANSPORT IN MEMBRANE

| | | |
|-------|--|----|
| 3.1 | Modelling in immunodiagnostic test kit | 57 |
| 3.2 | Membrane diffusion study: Fick's Law | 58 |
| 3.3 | Measurement of diffusion coefficients | 60 |
| 3.3.1 | Diffusion cell | 63 |
| 3.4 | Mathematic modelling for diffusion in lateral flow NC membrane | 64 |
| 3.4.1 | Model assumption | 65 |
| 3.4.2 | Model development | 66 |
| 3.4.3 | Evaluation of the lateral hindered diffusion coefficient | 72 |

CHAPTER 4 – MATERIALS AND METHODS

| | | |
|-----------|--|-----|
| 4.1 | Overall experimental flowchart | 75 |
| 4.2 | Materials and chemicals | 77 |
| 4.3 | Membrane preparation method | 78 |
| 4.3.1 | Preparation of casting solution | 78 |
| 4.3.2 | Membrane casting process | 79 |
| 4.3.3 | Statistical analysis: Crossed Mixture-Process design | 81 |
| 4.4 | Characterization of lateral flow NC membrane | 84 |
| 4.4.1 | Membrane porosity | 84 |
| 4.4.2 | Pore size distribution | 85 |
| 4.4.3 | Field Emission Scanning Electron Microscope (FESEM) | 85 |
| 4.4.4 | Attenuated Total Reflectance Fourier Transform Infrared (ATR-FTIR) | 86 |
| 4.4.5 | Atomic Force Microscope (AFM) | 86 |
| 4.4.6 | Densitometer | 87 |
| 4.5 | Modification of membrane morphology: thermal-mechanical stretching | 88 |
| 4.5.1 | Design of membrane stretcher | 88 |
| 4.5.1 (a) | Stretching platform | 89 |
| 4.5.1 (b) | Membrane rigid support beams | 90 |
| 4.5.1 (c) | Thermal control system | 91 |
| 4.5.1 (d) | Electric stepper motor | 91 |
| 4.5.1 (e) | Digital stretching length counter | 93 |
| 4.5.2 | Stretching of lateral flow NC membrane | 94 |
| 4.5.2 (a) | Setting of stretching temperature | 95 |
| 4.5.2 (b) | Setting of stretching rate | 96 |
| 4.5.2 (c) | Setting of stretching elongation | 96 |
| 4.5.3 | Statistical analysis: design experiment for stretching parameters | 96 |
| 4.6 | Performance evaluation of membrane | 98 |
| 4.6.1 | Membrane protein binding capacity | 98 |
| 4.6.2 | Lateral wicking time | 99 |
| 4.6.3 | Dot staining | 100 |
| 4.6.3 (a) | Settings of protein dot concentration | 101 |
| 4.6.3 (b) | Settings of protein dot volume | 101 |

| | | |
|-------|---|-----|
| 4.7 | Performance evaluation in immunochromatography testing | 101 |
| 4.7.1 | Assembly of diagnostic kit | 102 |
| 4.7.2 | Diagnostic testing method | 103 |
| 4.8 | Mathematical modeling for lateral hindered diffusion in NC membrane | 104 |
| 4.8.1 | Preparation of membrane and diffusing solution | 104 |
| 4.8.2 | Stokes diaphragm diffusion cell | 105 |
| 4.8.3 | Solute diffusion experiments | 106 |

CHAPTER 5 – SYNTHESIS, CHARACTERIZATION AND MODIFICATION

| | | |
|-----------|---|-----|
| 5.1 | Synthesis of lateral flow NC membrane | 108 |
| 5.1.1 | Effects of casting formulation | 109 |
| 5.1.1 (a) | Effects of NC polymer on lateral flow membrane performance | 109 |
| 5.1.1 (b) | Effects of additive on lateral flow membrane performance | 116 |
| 5.1.1 (c) | Effects of water as pore former on lateral flow membrane performance | 124 |
| 5.1.2 | Effects of casting conditions | 132 |
| 5.1.2 (a) | Effects of casting thickness on lateral flow membrane performance | 132 |
| 5.1.2 (b) | Effects of temperature on lateral flow membrane performance | 138 |
| 5.2 | Crossed-Mixture-Process design for interaction between membrane formulations and casting conditions | 143 |
| 5.2.1 | ANOVA and regression analysis | 144 |
| 5.2.2 | Diagnostic statistic | 151 |
| 5.2.3 | Model graph and surface contour plot | 154 |
| 5.2.4 | Process verification | 159 |
| 5.3 | Modification of membrane morphology | 160 |
| 5.3.1 | Characteristics of stretched and un-stretched membranes | 161 |
| 5.3.1 (a) | FESEM | 161 |
| 5.3.1 (b) | Porosity, pore size ratio and thickness | 163 |
| 5.3.1 (c) | AFM | 165 |

| | | |
|-------|--|-----|
| 5.3.2 | Effects of elongation on lateral flow membrane performance | 166 |
| 5.3.3 | Effects of temperature on lateral flow membrane performance | 168 |
| 5.3.4 | Effects of stretching rate on lateral flow membrane performance | 170 |
| 5.3.5 | Summary of stretching effects on membrane performance | 172 |
| 5.4 | Response Surface Analysis (RSM) for membrane modification through thermal mechanical stretching techniques | 173 |
| 5.4.1 | Membrane porosity | 174 |
| 5.4.2 | Membrane binding ability | 176 |
| 5.4.3 | Lateral wicking time | 179 |
| 5.4.4 | Verification on statistical models and diagnostic statistic | 181 |
| 5.4.5 | Optimization and verification | 186 |

CHAPTER 6 – PERFORMANCE EVALUATION AND MODELING

| | | |
|-------|--|-----|
| 6.1 | Membrane performance on dot staining | 190 |
| 6.1.1 | Effects of protein concentration | 192 |
| 6.1.2 | Effects of protein volume | 195 |
| 6.2 | Membrane performance as immunoassay | 199 |
| 6.2.1 | Binding ability | 199 |
| 6.2.2 | Lateral wicking time | 204 |
| 6.3 | Modeling for lateral hindered diffusion in NC membrane | 206 |
| 6.3.1 | Lateral diffusion properties for NC membrane | 207 |
| 6.3.2 | Parameter estimation | 208 |
| 6.3.3 | Model verification | 211 |

CHAPTER 7 – CONCLUSIONS, RECOMMENDATIONS AND FUTURE DIRECTIONS

| | | |
|-----|-------------------|-----|
| 7.1 | Conclusions | 216 |
| 7.2 | Recommendations | 220 |
| 7.3 | Future directions | 222 |

| | | |
|---------------------|--|------------|
| BIBLIOGRAPHY | | 223 |
|---------------------|--|------------|

| | |
|---|-----|
| APPENDICES | 240 |
| Appendix A Calibration Curves | 241 |
| Appendix B Curve Fitting of erf α versus α | 242 |
| Appendix C Curve Fitting of α versus α (erf ($\alpha/2$)) | 244 |
| Appendix D MATLAB Functions for Solving Lateral Flow Diffusion Model | 247 |
| Appendix E Model development for diffusion in lateral flow NC membrane | 250 |
| | |
| LIST OF PUBLICATIONS AND AWARDS | 252 |

LIST OF TABLES

| | | Page |
|-----------|--|------|
| Table 2.1 | Membrane pore size versus solutes separation in membrane processes (Cheryan, 1998) | 17 |
| Table 2.2 | Preparation methods of synthetic membrane (Cheryan, 1998; Kesting, 1985; Mulder, 2003) | 26 |
| Table 2.3 | Membrane modification methods | 39 |
| Table 3.1 | Common methods to measure diffusion coefficient (Cussler, 1997) | 61 |
| Table 4.1 | List of materials and chemicals used | 77 |
| Table 4.2 | Design layout and responses for mixture-process crossed-design | 81 |
| Table 4.3 | Design layout of different stretching settings for membrane morphology modification | 95 |
| Table 4.4 | Design layout and experimental responses for central composite design | 97 |
| Table 4.5 | Independent variables and their coded and actual values used in the response surface study | 98 |
| Table 4.6 | Physical data for BSA and Lysozyme | 105 |
| Table 5.1 | Chapter content summary for synthesis, characterization and modification | 109 |
| Table 5.2 | Various concentrations of NC polymer in membrane casting dope | 110 |
| Table 5.3 | Effects of polymer concentration on membrane pore size, porosity and thickness | 112 |
| Table 5.4 | Membrane casting compositions | 117 |
| Table 5.5 | Water content in membrane casting dope | 124 |
| Table 5.6 | Effects of drying temperature on membrane pore size, porosity and thickness | 138 |
| Table 5.7 | Responses for Crossed Mixture-Process Design | 143 |

| | | |
|------------|---|-----|
| Table 5.8 | ANOVA, variance analysis and regression model from the crossed design for membrane protein binding ability | 146 |
| Table 5.9 | ANOVA, variance analysis and regression model from the crossed design for membrane wicking time analysis | 146 |
| Table 5.10 | ANOVA and variance analysis for membrane protein binding ability | 150 |
| Table 5.11 | ANOVA and variance analysis for membrane wicking time analysis | 150 |
| Table 5.12 | Numerical optimization and verification for mixture-process crossed design | 159 |
| Table 5.13 | Verification between predicted values from model and actual values from experiment | 160 |
| Table 5.14 | Characterization of membrane after stretched | 164 |
| Table 5.15 | R_{RMS} and R_a roughness for stretched and un-stretched membrane | 166 |
| Table 5.16 | Design layout and experimental responses for central composite design | 174 |
| Table 5.17 | ANOVA and variance analysis for porosity model and model terms | 176 |
| Table 5.18 | Summary of ANOVA and regression analysis for membrane porosity | 176 |
| Table 5.19 | ANOVA and variance analysis for protein binding model and model terms | 179 |
| Table 5.20 | Summary of ANOVA and regression analysis for membrane protein binding ability | 179 |
| Table 5.21 | ANOVA and variance analysis for wicking time model and model terms | 181 |
| Table 5.22 | Summary of ANOVA and regression analysis for wicking time of membrane | 181 |
| Table 5.23 | Numerical optimization for central composite design | 188 |
| Table 5.24 | Confirmation between optimized stretching settings calculated from mathematical design and experimental study | 189 |

| | | |
|-----------|---|-----|
| Table 6.1 | Wicking time for target analyte and gold conjugate to bind on the membrane capture zone | 205 |
| Table 6.2 | Experimental diffusion coefficients with respect to various pore sizes of membranes | 208 |
| Table B.1 | The Error Function | 242 |
| Table C.1 | Values of α , $\alpha/2$ and $(\text{erf}(\alpha/2))$ | 244 |

LIST OF FIGURES

| | | Page |
|------------|--|------|
| Figure 1.1 | Relationship between market demands and membrane developments | 2 |
| Figure 1.2 | Schematic of porous membrane with random oriented polymer matrix (Cheryan, 1998) | 3 |
| Figure 1.3 | Filtration spectrum (Kosh-Membrane-Systems, 2004) | 4 |
| Figure 2.1 | Chemical structure of nitrocellulose polymer | 20 |
| Figure 2.2 | Phase inversion techniques | 27 |
| Figure 2.3 | Schematic diagram for dry phase inversion | 29 |
| Figure 2.4 | Schematic diagram of stretching mechanism | 44 |
| Figure 2.5 | Preparation of immunochromatography device (side view) | 50 |
| Figure 2.6 | Basic principle of diagnostic test strip | 51 |
| Figure 2.7 | Bonding mechanism between protein and nitrocellulose membrane: (a) chemical structure of protein (b) chemical structure of nitrocellulose (c) dipole of peptide bonds in protein (d) dipole of nitrate group in membrane | 52 |
| Figure 2.8 | Protein band width as a function of liquid contact zone: (a) wide contact (b) intermediate contact (c) narrow contact of the protein solution on the membrane surface. (Millipore-Corporation, 2002) | 54 |
| Figure 3.1 | Diaphragm cell (Cussler, 1997) | 63 |
| Figure 3.2 | Schematic of the partially blocked membrane | 66 |
| Figure 3.3 | Schematic of the concentration gradient across the membrane layer | 67 |
| Figure 4.1 | Flowchart of overall experimental works | 76 |
| Figure 4.2 | Mixing flask for casting solution | 79 |
| Figure 4.3 | Lateral Flow Immunoassay (A: Top view of the immunoassay strip, B: Side view of the immunoassay strip) | 103 |
| Figure 4.4 | Diagram of diffusion cell | 105 |

| | | |
|-------------|---|-----|
| Figure 5.1 | ATR-FTIR spectra of (a) commercial membrane (Millipore HF 240) and (b) synthesised membrane | 111 |
| Figure 5.2 | Wicking time needed for testing medium (a) Water (b) Phenol red to migrate 4cm heights along the membrane strips prepared at different polymer concentrations | 115 |
| Figure 5.3 | Effects of casting polymer composition on membrane protein binding ability | 116 |
| Figure 5.4 | Effects of different additives on the membrane porosity | 118 |
| Figure 5.5 | Schematic drawing of phase inversion at the SHS concentration (a) below CMC (b) above CMC | 119 |
| Figure 5.6 | Effects of different additives on lateral flow wicking times (s) for 4cm of migration length | 121 |
| Figure 5.7 | Effects of different additives on the membrane protein-binding ability | 122 |
| Figure 5.8 | Effects of water content on membrane porosity and pore size | 125 |
| Figure 5.9 | Histograms of pore size distributions for membranes formed by (a) 1.5, (b) 3.5, and (c) 5.5 wt. % of water content in casting solutions | 126 |
| Figure 5.10 | Wicking time needed for the testing medium (distilled water and phenol red) to migrate along the vertical height of membrane strip: (a) 2 cm and (b) 4 cm | 129 |
| Figure 5.11 | Effect of water content on membrane protein-binding ability | 131 |
| Figure 5.12 | Variation in pore size (μm) and porosity (%) of NC membranes prepared with different cast thicknesses | 135 |
| Figure 5.13 | Wicking rate for nitrocellulose membrane with increased distances of membrane strip after initial contact between the membrane and deionised water (test medium) | 136 |
| Figure 5.14 | Variation in membrane cast thickness to protein binding capacity of nitrocellulose membrane (Initial BSA concentration = 3000 ppm) | 137 |
| Figure 5.15 | Wicking time needed for testing medium (a) Water (b) Phenol red to migrate 4cm height along the membrane strips prepared at different drying temperature (27 °C, 40 °C and 50 °C) | 141 |
| Figure 5.16 | Effects of drying temperature on the membrane protein binding ability | 142 |

| | | |
|-------------|---|-----|
| Figure 5.17 | The interactions between cast solutions and drying temperature for membrane protein binding ability. 1 = run 1 & 3, 2 = run 13 & 43, 3 = run 28 & 34, 4 = run 44 & 47, 5 = run 39 & 49, 6 = run 52 & 10, 7 = run 4 & 37, 8 = run 12 & 38, 9 = run 50 & 30, 10 = run 21 & 31 | 147 |
| Figure 5.18 | The interactions between cast solutions and evaporation time for membrane protein binding ability. 1 = run 4 & 53, 2 = run 33 & 36, 3 = run 2 & 31, 4 = run 55 & 13, 5 = run 19 & 48, 6 = run 39 & 35, 7 = run 25 & 44, 8 = run 34 & 15, 9 = run 54 & 29, 10 = run 41 & 30, 11 = run 3 & 40, 12 = run 23 & 52 | 148 |
| Figure 5.19 | Diagnostic plots for membrane protein binding regression model for (a) normal distribution analysis, (b) residuals versus predicted, (c) box-cox and (d) actual versus predicted | 152 |
| Figure 5.20 | Diagnostic plots for membrane wicking time regression model for (a) normal distribution analysis, (b) residuals versus predicted, (c) box-cox and (d) actual versus predicted | 153 |
| Figure 5.21 | 3D surface contour plots for membrane protein binding ($\mu\text{g}/\text{cm}^3$) at different cast solution and evaporation time (a) 0 min, (b) 2.5 min and (c) 5 min | 155 |
| Figure 5.22 | 3D surface contour plots for membrane wicking speed (s/4cm) at different cast solution and drying temperature of (a) 27 °C, (b) 33.5 °C and (c) 40 °C | 156 |
| Figure 5.23 | 3D (left) and 2D (right) contour plots for protein binding of membrane formed at different process factors and polymer content of (a) 4 wt.%, (b) 4.5 wt.% and (c) 5 wt.% | 158 |
| Figure 5.24 | AFM micrographs for surfaces of (a) un-stretched membrane and (b) stretched membrane with 18% of elongation | 165 |
| Figure 5.25 | Effects of stretching elongation on membrane lateral wicking time (to migrate 4cm height along the membrane strip and each value represents an average value of 3 data) | 167 |
| Figure 5.26 | Effects of stretching elongation on membrane protein binding ability (each value represents an average value of 3 data) | 168 |
| Figure 5.27 | Effects of stretching temperature on membrane lateral wicking time (to migrate 4cm height along the membrane strip and each value represents an average value of 3 data) | 169 |
| Figure 5.28 | Effects of stretching temperature on membrane protein binding ability (each value represents an average value of 3 data) | 170 |

| | | |
|-------------|---|-----|
| Figure 5.29 | Effects of stretching rate on membrane lateral wicking time (to migrate 4cm height along the membrane strip and each value represents an average value of 3 data) | 171 |
| Figure 5.30 | Effects of stretching rate on membrane protein binding ability (each value represents an average value of 3 data) | 172 |
| Figure 5.31 | Response surface plotted on (a) stretching elongation: stretching temperature, (b) stretching rate: stretching temperature for membrane porosity | 175 |
| Figure 5.32 | Response surface plotted on (a) stretching elongation: stretching temperature, (b) stretching rate: stretching temperature for membrane protein binding ability | 177 |
| Figure 5.33 | Response surface plotted on (a) stretching elongation: stretching temperature, (b) stretching rate: stretching temperature for membrane lateral wicking time | 180 |
| Figure 5.34 | Interaction via stretching temperature: stretching rate (▲ for 0.1 mm/s, ■ for 0.04 mm/s) and stretching elongation at 13% (● design points) | 182 |
| Figure 5.35 | Normal probability plot of residual for membrane (a) porosity (b) protein binding ability (c) lateral wicking time | 183 |
| Figure 5.36 | Plot of residual versus predicted response for membrane (a) porosity (b) protein binding ability (c) lateral wicking time | 184 |
| Figure 5.37 | Predicted vs. actual values plot for (a) membrane porosity; (b) membrane protein binding ability; (c) membrane lateral wicking time | 185 |
| Figure 5.38 | Response surface plot of the desirability operating region over stretching temperature: stretching rate at stretching elongation set at 18% | 186 |
| Figure 5.39 | Overlay plot of the desirability operating region for membrane stretching operation | 187 |
| Figure 6.1 | Colour densities for stained protein dots at increasing concentration of BSA at constant volume (1 µl per spot), where each protein dot value represents an average value of 6 spots (a: 0.1 - 5 mg/ml per spot, b: 5 - 20 mg/ml per spot) | 193 |
| Figure 6.2 | Densitometry dot area percentage (100 % of area percentage referred to measuring aperture with diameter of 3mm or area 7.07 mm ²) at increasing concentration of BSA with constant volume of 1 µl per spot. (a: 0.1-5 mg/ml per spot, b: 5-20 mg/ml per spot) | 194 |

| | | |
|-------------|--|-----|
| Figure 6.3 | Colour densities for stained protein dots at increasing volume of BSA at constant concentration (20 mg/ml), where each protein dot value represents an average value of 5 spots | 197 |
| Figure 6.4 | Densitometry dot area percentage (100 % of area percentage referred to measuring aperture with diameter of 3mm or area 7.07 mm ²) at increasing volume of BSA with constant concentration of 20 mg/ml | 198 |
| Figure 6.5 | Concentration of BSA as a function of time. Initial BSA concentration = 10 mg/ml, pH: 7, lateral diffusion length of 2cm and temperature of 25 °C | 207 |
| Figure 6.6 | Interpolation of observed D_e for different membranes of varying pore sizes (BSA concentration of 10 mg/ml and lateral diffusion length of 2cm) | 210 |
| Figure 6.7 | Diffusion model and experiment results for 10mg/ml of BSA at pH 7, temperature of 25 °C, diffusion length of 2cm, membrane pore size of 5 μm and D_e of $1.0735 \times 10^{-8} \text{ m}^2/\text{s}$ | 212 |
| Figure 6.8 | Diffusion model and experiment results for 10mg/ml BSA, pH 7, temperature 25 °C, diffusion length of 1 cm, membrane pore size of 4.9 μm and D_e of $1.6909 \times 10^{-8} \text{ m}^2/\text{s}$ | 213 |
| Figure 6.9 | Diffusion model and experiment results for 10mg/ml BSA, pH 7, temperature 25 °C, diffusion length of 3 cm, membrane pore size of 7.5 μm and D_e of $1.7126 \times 10^{-8} \text{ m}^2/\text{s}$ | 214 |
| Figure 6.10 | Diffusion model and experiment results for 10mg/ml BSA and Lysozyme at pH 7, temperature 25 °C, diffusion length of 1cm and membrane pore size of 4.9 μm (D_e for BSA = $8.4544 \times 10^{-9} \text{ m}^2/\text{s}$ and D_e for Lysozyme = $1.4104 \times 10^{-8} \text{ m}^2/\text{s}$) | 215 |
| Figure A.1 | Calibration curve of BSA concentration and absorbance | 241 |
| Figure A.2 | Calibration curve of Lysozyme concentration and absorbance | 241 |
| Figure B.1 | Curve fitted line of erf α versus α | 243 |
| Figure C.1 | Curve fitted line of α versus $\alpha(\text{erf}(\alpha/2))$ for $(\alpha/2)$ ranging from 0 to 2.8 | 245 |
| Figure C.2 | Curve fitted line of α versus $\alpha(\text{erf}(\alpha/2))$ for $(\alpha/2)$ more than 2.8 | 246 |

LIST OF PLATES

| | | Page |
|-----------|--|------|
| Plate 2.1 | SEM image showing the pattered structure of the membrane produced by the uni-axially stretching operation (Kurumada et al., 1998) | 43 |
| Plate 2.2 | SEM image showing the pattered structure of the membrane produced by the bi-axially stretching operation (Kurumada et al., 1998) | 43 |
| Plate 4.1 | Membrane auto casting machine | 80 |
| Plate 4.2 | Membrane stretcher | 89 |
| Plate 4.3 | Stretching platform | 90 |
| Plate 4.4 | Membrane rigid support beams | 90 |
| Plate 4.5 | Thermal control system | 91 |
| Plate 4.6 | Electric stepping motor | 92 |
| Plate 4.7 | Stepping controller | 93 |
| Plate 4.8 | Digital stretching length counter | 94 |
| Plate 4.9 | Diagnostic test kit | 102 |
| Plate 5.1 | FESEM micrographs of membrane surface structure (left) and thickness (right) for NC polymer contents of (a,d) 4.0, (b,e) 5.0, and (c,f) 6.0 wt % in casting solutions | 113 |
| Plate 5.2 | FESEM micrographs of membrane surface structure, with water contents (wt %) of (a) 1.5, (b) 3.5, and (c) 5.5 | 127 |
| Plate 5.3 | FESEM micrographs for the surfaces (a - c) (2000 \times) and cross-sections (d - f) (1000 \times) of NC membranes, prepared with cast thickness of: (a, d) 600 μm , (b, e) 700 μm , and (c, f) 800 μm | 133 |
| Plate 5.4 | FESEM micrographs of membrane surface structure for: (a) 27 $^{\circ}\text{C}$, (b) 40 $^{\circ}\text{C}$, and (c) 53 $^{\circ}\text{C}$ of drying temperature | 140 |
| Plate 5.5 | FESEM micrographs for the surfaces of (a) un-stretched and (b) stretched membranes, prepared with stretching elongation of 22% of total membrane sample. Arrow: the stretching direction | 162 |

| | | |
|-----------|--|-----|
| Plate 5.6 | FESEM micrographs for the surfaces of stretched membrane prepared at (a) 35 °C and (b) 65 °C of stretching temperature (stretching elongation: 10% of total membrane sample and stretching rate: 0.04mm/s). | 163 |
| Plate 6.1 | Stained BSA protein dots (immobilized protein volume: 1µl) on NC membrane with varying protein concentrations (a:0.1mg/ml, b:0.5mg/ml, c:1mg/ml, d:2mg/ml, e:3mg/ml, f:4mg/ml, g:5mg/ml, h:10mg/ml, i:15mg/ml and j:20mg/ml) | 191 |
| Plate 6.2 | Stained protein dots (immobilized protein concentration: 20 mg/ml) on NC membrane with varying protein volumes (a:0.5µl, b:1.0µl, c:1.5µl, d:2µl, e:2.5µl, f:3µl) | 195 |
| Plate 6.3 | Interpretation of protein binding via sharpness and wideness of the protein lines on membrane surface, where the commercial membranes included: Lane 1 (HF060), Lane 2 (HF135) and Lane 3 (HF240), while the synthesised membranes included Lane 4 (sample 15), Lane 5 (sample 5) and Lane 6 (sample 13) | 201 |
| Plate 6.4 | Width of the protein lines with different membrane pores. Lane 1: HF060; Lane 2: HF135; Lane 3: HF240; Lane 4: sample 15 | 202 |
| Plate 6.5 | Interpretation of bad protein binding via sharpness of the protein lines on membrane surface | 203 |

LIST OF ABBREVIATION

| | |
|----------|---|
| Ab | Antibody |
| AFM | Atomic force microscopy |
| Ag | Antigen |
| ATR-FTIR | Attenuated total reflectance-fourier transform infrared |
| BCA | Bicinchoninic acid working reagent |
| BSA | Bovine serum albumin |
| CCD | Central composite design |
| CMC | Critical micelle concentration |
| DF | Degree of freedom |
| DNA | Deoxyribonucleic acid |
| DOE | Design of experiment |
| E | Ethanol |
| EIA | Enzyme immunosorbent assay |
| FESEM | Field emission scanning electron microscope |
| ICT | Intracellular transport buffer |
| IgG | Immunoglobulin G |
| IP | Isopropanol |
| IPN | Interpenetrating polymer network |
| MA | Methyl acetate |
| MDSC | Modulated differential scanning calorimetry |
| MF | Microfiltration |
| N | Nitrate |
| NC | Nitrocellulose |
| PAPI | Phosphate buffer saline |
| PBS | Polymer assisted phase inversion |
| PEG | Poly(ethylene glycol) |
| PES | Polyethersulfone |
| ppm | Parts per million |
| PVDF | poly(vinylidene) fluoride |
| PTFE | polytetrafluoroethylene |
| RO | Reverse osmosis |

| | |
|----------|---|
| rpm | Rotation per minute |
| RH | Relative humidity |
| RMS | Root mean square |
| RSM | Response surface methodology |
| SHS | Sodium hexadecane sulfonate |
| SDS-PAGE | Sodium dedecyl sulfate polyacrylamide gel electrophoresis |
| SS | Sum of Squares |
| MS | Mean Square |
| TIPS | Thermal induced phase separation |
| UF | Ultrafiltration |
| VIPS | Vapour induced phase separation |

LIST OF SYMBOLS

| | | Unit |
|----------------------|--|--------------|
| A | Membrane diffusion area | m^2 |
| $Adj-R^2$ | Adjusted coefficient of determination | - |
| c_i | Solute concentration | kg/m^3 |
| C | Solute concentration when $z > 0$ | $\mu g/ml$ |
| C_{in} | Solute concentration at membrane wall of donor chamber | $\mu g/ml$ |
| C_{out} | Solute concentration at membrane wall of receptor chamber | $\mu g/ml$ |
| dC | Solute concentration different in diffusion length | $\mu g/ml$ |
| dt | Diffusion time difference | s |
| dz | Axial direction difference | m |
| D | Diffusion coefficient of solute | m^2/s |
| D_e | Effective diffusion coefficient | m^2/s |
| D_f | Desirability function in RSM | - |
| D_o | Predicted diffusion coefficient in dilute solution | m^2/s |
| D_p | Membrane pore diameter | μm |
| d_i | partial desirability function for specific response in RSM | - |
| e | Error estimation | - |
| F | Thermodynamic force | $kg.m/s^2$ |
| F_f | Frictional resistance | $kg.m/s^2$ |
| $f(x_1, x_2, \dots)$ | Mixture variables | - |
| $g(z_1, z_2, \dots)$ | Casting process factors | - |
| h_o | $\frac{\partial C}{\partial \eta}$ at constant volume | $\mu g/ml$ |
| J | Solute flux | $kg/(m^2.s)$ |
| k_B | Boltzmann's constant, 1.38×10^{-23} | J/K |
| L_1 | Major axis length | μm |
| L_2 | Minor axis length | μm |

| | | |
|-------------|--|-----------------|
| Log D | Absorbance of colour density in densitometer | - |
| MW | Molecular weight | g/mol |
| N | Number of experiments required/ data point | - |
| N_A | Avogadro's number | 1/mol |
| N_s | Number of stepping step | - |
| Pred- R^2 | Predicted coefficient of determination | - |
| R_a | Mean roughness of membrane | nm |
| R_o | Molecular radius | m |
| R_p | Membrane pore radius | m |
| R_{RMS} | RMS roughness of membrane | nm |
| R_s | Stoke's radius of solute molecular | m |
| R^2 | Coefficient of determination | - |
| r_i | importance of particular response in RSM | - |
| S | Specific scan area | nm ² |
| T | Transmittance | % |
| T | Operating temperature | K |
| t | Time | s |
| t_o | Initial Time | s |
| t_s | Time of a stretching step | s |
| t^* | Non-dimensional variable of time, define $t^* = \frac{t}{t_o}$ | - |
| V_A | Apparent volume of membrane | cm ³ |
| V_E | Existent volume of membrane | cm ³ |
| V_{in} | Solution volume in the donor chamber | m ³ |
| V_{out} | Solution volume in the receptor chamber | m ³ |
| v | Velocity | m/s |
| v_e | Stretching rate | µm/s |
| Y | Predicted response | - |
| z | Length of diffusion | m |
| z_o | Initial length of diffusion | m |

| | | |
|-------|---|----|
| z_m | Mean height value of scan sample by AFM | nm |
| z^* | Non-dimensional variable of diffusion length, define $z^* = \frac{z}{z_o}$ | - |

Greek letters

| | | |
|---------------|---|-------------------|
| θ | Pore aspect ratio | - |
| ϕ | Polymer Fraction | - |
| ξ | Ratio of the solute radius and membrane pore radius ($\xi = \frac{R_s}{R_p}$) | - |
| ε | Porosity of membrane | % |
| λ | Wavelength | nm |
| λ_L | Lamda value | - |
| β_o | Plane interception coefficient | - |
| β_x | Partial regression coefficient | - |
| β | Constant of diaphragm cell | 1/cm ² |
| ℓ_e | Stretching elongation | mm |
| φ | Dot area scanned by densitometer | % |
| π | Constant value of 3.14159 | - |
| α | Ration of system length to diffusion distance, Defined by $\alpha = \frac{L}{\sqrt{D_e t}}$ | - |
| η | Ratio of total system length to diffusion distance, Defined by $\eta = \frac{z}{\sqrt{D t}}$ | - |
| μ | Dynamic viscosity | Pa.s |
| ρ | Density | kg/m ³ |
| $erf\alpha$ | Value of error function | - |

MEMBRAN NITROSELULOSA ALIRAN SISI BAGI KEGUNAAN KIT DIAGNOSIS: SINTESIS, PENCIRIAN DAN PENILAIAN PRESTASI

ABSTRAK

Membran nitroselulosa (NC) aliran sisi merupakan salah satu keperluan utama dalam bidang bioperubatan kerana keupayaan pengikatannya yang baik, ciri-ciri pembasahan yang tinggi dan tahap penompokan belakang yang rendah. Walau bagaimanapun, masih terdapat banyak cabaran dalam kaedah pembuatan membran untuk mensintesis dan mengawal morfologi membran bagi memenuhi keperluan keseluruhan aplikasi imunoasai (immunoassay), di mana ia merupakan fokus utama penyelidikan ini. Dalam penyelidikan ini, membran NC aliran sisi telah berjaya dihasilkan melalui penyongsangan fasa kering. Kajian terperinci mengenai kesan formulasi (polimer, pemilihan bahan tambahan dan kepekatan serta fungsi air sebagai pembentuk liang) dan keadaan proses (ketebalan dan suhu pengeringan) telah dijalankan. Perubahan morfologi dan ciri-ciri membran telah dianalisa dan dikategorikan dalam kumpulan berfungsi, keporosan, saiz liang, taburan saiz liang, kekasaran permukaan, ketebalan berkesan, masa sisi penyumbuan (wicking) bagi keupayaan pengikatan protein dan masa sisi penyumbuan cecair untuk memahami ciri-ciri dan kualiti membran yang telah disintesis. Dalam kajian ini, membran-membran dengan diameter liang minimum dari 1.3 hingga 7.5 μm boleh dihasilkan dengan mudah dengan mengenalpasti interaksi-interaksi yang terlibat antara formulasi yang didapati dan pembolehubah-pembolehubah proses acuan. Reka bentuk campuran proses berpaling telah menunjukkan formulasi acuan optimum dengan mempertimbangkan faktor-faktor proses sebagai: 4% berat NC, 82% berat pelarut (5:3 nisbah MA:E), 10% berat IP, 2% berat air dan 2% berat gliserol pada

suhu pengeringan 27°C dan masa penyejatan selama 3.05 minit. Kajian ini juga mendemonstrasikan pengubahsuaian morfologi membran melalui teknik regangan unipaksi terma mekanikal. Berdasarkan keputusan ujikaji kesan regangan, keputusan eksperimen, analisa AFM dan FESEM menunjukkan dengan jelas bahawa morfologi membran telah diubah suai akibat kesan regangan (pemanjangan, suhu dan kadar regangan). Seperti yang diramal oleh reka bentuk komposit pusat (CCD) kaedah permukaan gerak balas (RSM), keadaan regangan optimum adalah pada 18 % pemanjangan, 35 °C suhu dan 0.07 mm/s kadar regangan, yang mana memberikan kadar aliran sisi tertinggi dan prestasi pengikatan masing-masing 579.0 s/4cm dan 4496.50 µg/cm². kajian prestasi membran bagi bintik protein dan immunoasai aliran sisi dijalankan setelah formulasi, keadaan acuan dan teknik pengubahsuaian telah didapati mempunyai kawalan yang baik dalam menghasilkan membran NC aliran sisi. Kajian bintik protein mendedahkan kesan kepekatan protein adalah penting dalam mempengaruhi ciri-ciri pengikat membran berbanding dengan kesan isipadu protein. Dalam immunoasai aliran sisi, prestasi keseluruhan membran yang disintesis adalah hampir sama dengan membran komersial (HF240), di mana ia telah menghasilkan satu garis pengikatan yang jelas dengan hanya 21 saat lebih lama dalam masa sisi penyumbuan. Model resapan sisi diperolehi dalam kajian ini telah ditentusahkan apabila data model dibanding dengan data ujikaji dengan nilai R² yang tinggi. Model yang dibangunkan adalah fleksibel dan teguh (robust), sesuai digunakan bagi resapan pelbagai dimensi dan juga sesuai untuk resapan Lysozyme.

LATERAL FLOW NITROCELLULOSE MEMBRANE FOR DIAGNOSTIC KIT APPLICATION: SYNTHESIS, CHARACTERIZATION AND PERFORMANCE EVALUATION

ABSTRACT

Lateral flow nitrocellulose (NC) membrane is one of the main requirements in the biomedical field due to its excellent binding capacity, high wetting properties and low background staining. However, there are still many challenges in the method of membrane fabrication in order to synthesise and control the membrane morphologies to fulfil the whole range of the required immunoassay applications, which is the main focus of this research. In this research, lateral flow NC membrane was successfully fabricated via dry phase inversion. Detailed studies on the effects of formulation (polymer, additive selection and concentration as well as the role of water as pore former) and process conditions (thickness and drying temperature) was carried out. The varied membrane morphologies and properties were examined and characterized in terms of functional group, porosity, pore size, pore size distribution, surface roughness, effective thickness, lateral wicking time of liquid and protein binding ability in order to comprehend the properties and qualities of synthesised membranes. In the study, membranes with mean pore diameter from 1.3 to 7.5 μm could be produced easily by identifying the interactions among the formulations and casting process variables. Crossed mixture-process design resulted in the optimum casting formulation by considering the process factors of: 4 wt.% of NC, 82 wt.% of solvents (5:3 ratio of MA:E), 10 wt.% of IP, 2 wt.% of water and 2 wt.% of glycerol at 27 °C of drying temperature and 3.05 min of evaporation time. The study also demonstrated the modification of membrane morphology via uniaxial thermal-mechanical stretching technique. Based on the result of the stretching effect

experiment, experimental results, AFM and FESEM analyses clearly showed that the membrane morphologies were modified by the stretching effects (elongation, temperature and stretching rate). As predicted by central composite design (CCD) of response surface methodology (RSM), the optimum stretching condition was found at 18 % of elongation, 35 °C of temperature and 0.07 mm/s of stretching rate, which gave the highest lateral flow rate and binding performances of 579.0 s/4cm 4496.50 $\mu\text{g}/\text{cm}^2$, respectively. Membrane performance in protein dot and lateral flow immunoassay were carried out after the said formulation, casting condition and modification technique were found to possess good control in producing lateral flow NC membrane. The protein dot study disclosed that protein concentration has a significant effect on the membrane binding properties compared to protein volume. In an lateral flow immunoassay, the overall performances of the synthesised membrane was in agreement with the commercial membrane (HF240), where it produced a sharper binding line with merely 21 second longer in lateral wicking time. The lateral diffusion model derived in this study was confirmed by the comparison of model data with that from the experiment with high R^2 values. The model is flexible and robust to be applied in different diffusion lengths and also well fitted to the diffusion of Lysozyme.

CHAPTER 1

INTRODUCTION

1.1 Membrane overview

Membrane can be described as the selective barrier between two phases, impermeable to specific particles or substances when exposed to the action of driving force (Zeman and Zydney, 1996; Cheryan, 1998). The relationship between the generated flow and the applied force is governed by the nature of the chemical substances and also by the membrane itself (Pinto *et al.*, 1999). Permeation through membranes can happen via convection, diffusion or electro migration, depending on either electrical potential, concentration, pressure or temperature gradient (Strathmann, 1990).

For the past three decades, technological advancement in membrane has attracted the attention of chemists, chemical and biotechnical engineers due to their unique separation principle, i.e. selective transport and efficient separation compared to other unit operations (Saxena *et al.*, 2009). Among various types of membranes, the polymeric membrane has led the market in membrane separation industries mainly because of its competitive performances and economics (Perry and Green, 1997). Nonetheless, selection of a suitable polymer for membrane synthesis is not a trivial task as specific membrane for specific application requires unique sets of characteristics, in terms of chain rigidity, chain interactions, stereo-regularity, and polarity of its functional groups (Zeman and Zydney, 1996). Besides, the polymer has to be competitively priced to comply with the low cost criteria of membrane separation process. The more commonly used polymers in membrane synthesis are

cellulose acetate, cellulose nitrate or nitrocellulose, polyamide, polyethersulfone (PES), polyacrylonitrile, and polyvinylidene fluoride (PVDF) (Zeman and Zydney, 1996).

Generally, research and development for membranes are market oriented depending on the needs and demands. By determining the quantitative relationship between membrane structure and its casting properties (i.e. formulation and casting condition), a fine polymer structure can be engineered to satisfy social requirements (Neogi, 1996). Flowchart in Figure 1.1 summarizes the relationship between social needs and the membrane development through the knowledge of membrane structure and its physical properties. As shown in Figure 1.1, consumer demand is initially transformed into membrane physical properties. From the required membrane physical properties, the membrane structure is designed. By governing the membrane fabrication method and its casting properties, membrane with specific characteristics and desired performances can be manufactured.

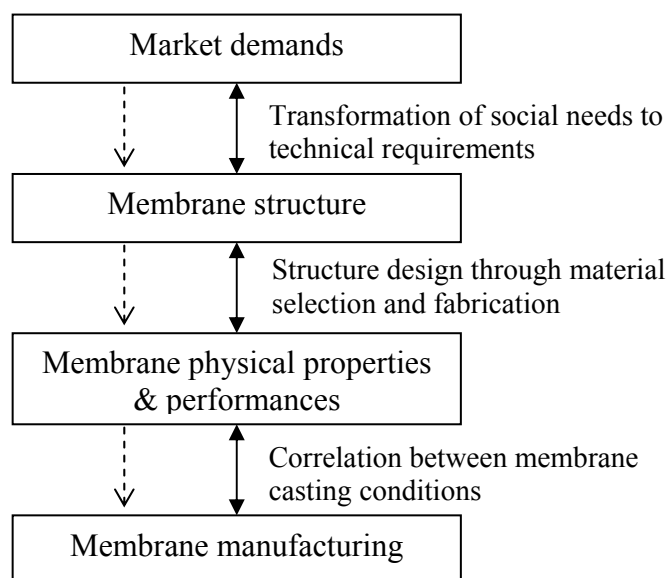


Figure 1.1: Relationship between market demands and membrane developments

1.2 Lateral flow nitrocellulose (NC) membrane

Similar to the microporous membrane, lateral flow NC membrane consists of a matrix of randomly oriented fibres or beads that are bonded together to form a tortuous maze of flow channels, as shown in Figure 1.2 (Cheryan, 1998). The separation of membrane is accomplished by size-exclusion mechanism in which both pore diameter and analyte size become the main parameters. In general, membrane is characterized by the pore size between 0.05 μm to about 12 μm . This range of pore size is very suitable to be used in microfiltration and well known for their effective properties to detect low concentration bacteria or viruses (Cheryan, 1998).



Figure 1.2: Schematic of porous membrane with random oriented polymer matrix (Cheryan, 1998)

One special feature of NC membrane is their high binding capacity and the large void volume between membrane pores. This binding affinity offers good accessibility for potential adsorption of protein molecules while the high pore connectivity contributes to rapid detection of analyte (Kung, 1991). Most of the membrane applications are based on the analytical protein blotting protocols, including protein immobilization, protein binding assays and lateral-flow

immuno-chromatography testing (Graf and Friedl, 1999; Beer *et al.*, 2002; Czerwinski *et al.*, 2005). This micro-pores membrane is capable of effectively removing red blood cell, bacteria as well as major pathogens and contaminants, as shown in Figure 1.3 (Kosh-Membrane-Systems, 2004).

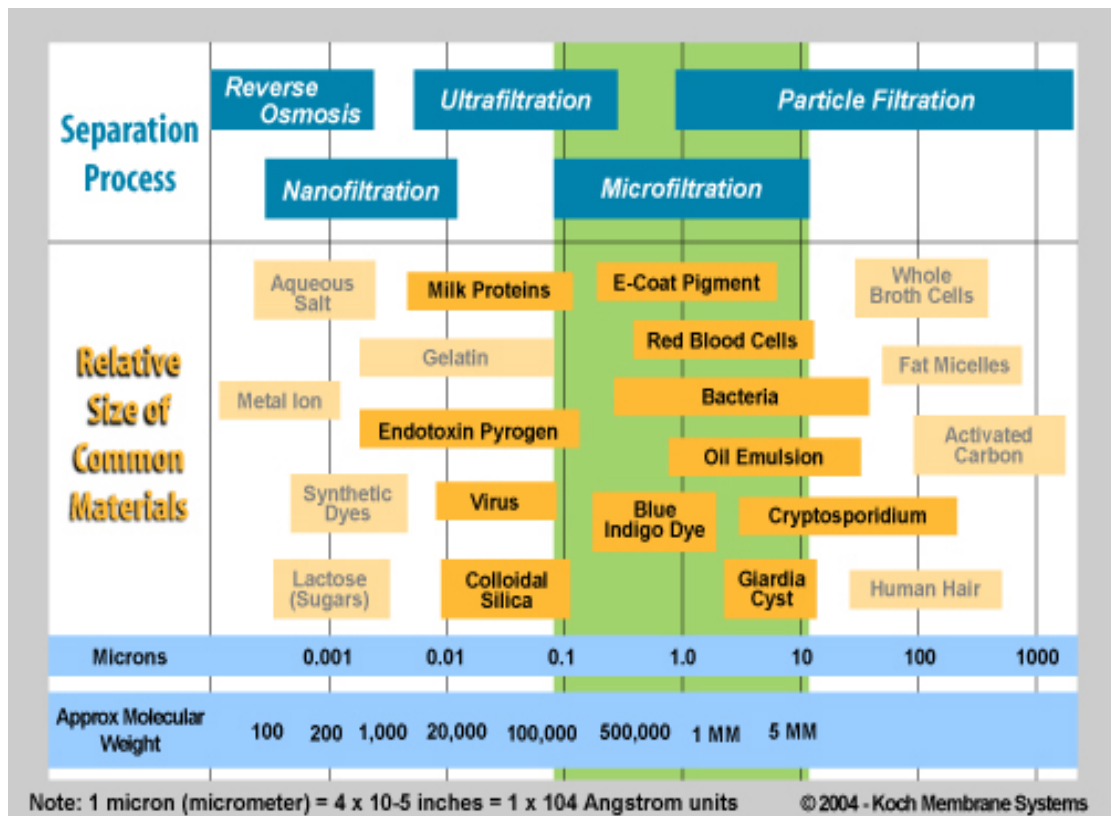


Figure 1.3: Filtration spectrum (Kosh-Membrane-Systems, 2004)

1.3 Lateral flow NC membrane for biomedical application

A large and growing number of membrane applications in biotechnology have been developed, where membrane modules are utilized for the collection of particles, particularly to meet the requirements of the bioprocess, food and pharmaceutical industries (Ali *et al.*, 2004; Sithigorngul *et al.*, 2007; van Reis and Zydney, 2007; Gui *et al.*, 2008). One of the most promising and potentially useful

applications of lateral flow membrane in biomedical is in the containment and metering device for controlled release of effectors such as drugs, fragrances, insecticides, and herbicides solutions (Saxena *et al.*, 2009).

The greatest sophistication in the exploitation of NC membranes as solid phase media is seen for pregnancy test kits. For such assays, a ligand specific for an analyte (normally, but not necessarily an antibody) is immobilized onto the membrane. Sample containing target analytes is solubilised with the detector agent and starts to move along the membrane strip. As the sample passes over the zone to which the capture reagent has been immobilized, the analyte-detector reagent complex is trapped. Colour developed proportionate to the amount of analytes is present in the sample (Zhang *et al.*, 2006).

1.4 Diagnostic kit

In the field of medical diagnostics, the major limitation associated with conventional diagnostic techniques is that it is time consuming and involves complex procedures. Hence, there has been a growing interest in developing low-cost techniques for accurate and rapid diagnosis of various diseases. These needs have prompted the exploration of the membrane materials that are able to execute the test in the most efficient and rapid way (Lonnberg and Carlsson, 2001; Qian and Bau, 2004).

Different membrane materials have intrinsic binding affinity for different proteins. For diagnostic kits, the highly desired features are excellent membrane binding capacity and the large void volume between membrane pore for rapid testing.

Physical and chemical attributes of membrane affect the lateral flow rate and binding properties, which in turn affects the reagent deposition, assay sensitivity, assay specificity and test line consistency in the diagnostic kit (Jones, 1999). Among the membranes used in the immunological analysis (such as nitrocellulose, nylon, polysulfone or certain acrylic co-polymers membrane), the lateral flow NC membrane has long occupied the position of central importance in diagnostics based on their ability to undergo size and/or charged protein separation with high purity and permeation (Lonnberg and Carlsson, 2001; Qian and Bau, 2004).

In recent years, the implementation of lateral flow diagnostics using adsorptive nitrocellulose (NC) membrane as chromatographic media is becoming more apparent (Czerwinski *et al.*, 2005). It has become a preferred diagnostic tool primarily because it eliminates the need for trained personnel and expensive equipment (Oku *et al.*, 2001; Qian and Bau, 2004). Additionally, storage and transportation at 4 °C are no longer required. The basis of all diagnostic kit is the antigen-antibody interactions among their large varieties of formats. Amid the diagnostic kit applications, enzyme immunosorbent assay (EIA) is the most common method due to its high sensitivity, specificity and reproducibility (Morais *et al.*, 1999).

Briefly, lateral flow diagnostic kit is a test strip made of a flat and highly porous membrane. A known antigen is immobilized at predetermined location (capture zone) along the porous membrane. Test sample containing target analyte is mixed with the buffer solution and reporting agent such as colloidal gold. This solution is then introduced into the membrane by capillary forces. As the solution

flows along the capture zone, the analyte and/or the reporting agent would bind onto the immobilized antigen (Oku *et al.*, 2001; Qian and Bau, 2004). The test result is clearly visible due to the appearance of red colour bands on the membrane strip. Development of colour is proportionate to the concentration of the bind analyte on the membrane surface. This technology is widely used in the hospital, laboratory medicine and life science research, to monitor infectious diseases in a more rapid and effective way.

1.5 Problem statement

Considerable amounts of past researches have revealed that nitrocellulose (NC) membrane contributes tremendously in the field of medical biotechnology. Although many studies have been done on characterizing the application buffers and application systems employed, the roles and effects of membrane are less likely to be fully investigated or optimised. Such an omission is often due to the fact that the latter element is frequently considered fixed even before the beginning of the development process, leaving little opportunity for changes to be made.

To achieve rapid disease detection using lateral flow diagnostics, the pores of NC membrane must be highly interconnected without sacrificing the physical strength of the membrane structure and its binding ability. The highly interconnected pores would hasten the lateral liquid flow rate in the membrane, due to the decrease in solute diffusion resistance across polymer matrix. However, these highly interconnected pores would reduce the membrane's mechanical strength and decrease the availability of total membrane surface area for protein binding affinity. Consequently, it will reduce the sharpness of the protein capture line on the

membrane surface. Therefore, there is an urgent need to optimise the membrane morphology, in order to enhance its lateral wicking rate without sacrificing the binding affinity of the membrane.

Unfortunately, development of lateral flow NC membrane remains a challenge, due to the lack of design methodology. Membrane fabrication techniques and the materials used are not disclosed by membrane developers. In membrane fabrication, chemical properties of polymer solutions and the casting conditions are closely associated with the membrane morphology. Different membrane structures provide for different lateral liquid flow rates and protein binding affinities. Hence, research focusing on membrane properties such as pore size, pore size distribution, effective thickness and porosity are urgently needed to determine the structure of membrane film and subsequently the membrane performance which no doubt, one day will become the key driver of the country's membrane technology.

The membrane morphology is difficult to control for the exact desired pore size due to the complex membrane formation parameters and processes. In order to produce membrane with a wide range of morphology, various formulations are required. This will ultimately result in high cost, lengthy research and development process. To produce the desired membrane, parameters used to control the membrane morphology need to be screened out in the first place. Extensive research on characterization and modification of the membrane can benefit the development of membrane design methods and facilitate their use in immunoassay application, which could then lead to the development of the whole new generation of NC membranes.

Although there are a number of membranes which can perform as transport medium in the diagnostic test strip, its application is almost universal to all kinds of diagnostic detection without much screening. The developed immunodiagnostic test strips are not able to cater for all applications, since different membrane materials, surface properties, structure and dimensions are required for a wide range of potential capture reagents. Thus, it is necessary to study the interrelationship between membrane morphology and performances of test strip, to meet the stringent requirements of diagnostic detection.

All these limitations, in truth, can be easily resolved if the knowledge and membrane formation techniques are improved and expanded.

1.6 Research objectives

The primary objective of this study is to develop a lateral flow membrane which consists of micro pores structure and capable for biomedical application. The present study has the following objectives:

- 1) To synthesise micro pores lateral flow nitrocellulose membranes for medical biotechnology application.
- 2) To study the correlations and to control the interconnections between environmental factors and formulations on membrane properties and performances.
- 3) To design and fabricate a membrane stretching machine to modify membrane morphology.

- 4) To investigate and optimize the effects of stretching parameters such as stretching rate, temperature and elongation on membrane properties and performances.
- 5) To study the performances of synthesized NC membranes on immunochromatography tests.
- 6) To model the lateral hindered diffusion of protein solutes (Lysozyme and BSA) in membrane and to validate the model from the experimental data.

1.7 Scope of study

In this study, techniques to produce lateral flow NC membrane using dry phase inversion method under controlled environment conditions were disclosed. In membrane formulation, the controlling parameters were polymer concentration, additive selection, additive (wetting agent) composition as well as concentration of pore former (water). Polymer concentration from 4 to 6 wt.% were used, to investigate the role of NC polymer in lateral flow immunochromatography testing. Investigations on the synthesised membranes with various wetting agents and pore formers (glycerol, SHS, PEG and water content) were carried out to identify the selection and concentration of the most suitable additive introduced into the casting solution. The water content studied was in the range from 1.5 to 5.5 wt.%. In the present study, membrane casting conditions such as drying temperature (27 to 53 °C) and casting thickness (600 to 800 um) had also been considered.

The membranes were characterized in terms of pore size, pore size distribution, porosity and effective thickness. Average pore sizes and thicknesses were measured using Field Emission Scanning Electron Microscope (FESEM), while

the membrane porosity was calculated through the correlation between membrane thickness, polymer weight and polymer density. The functional group of the synthesised membrane was further confirmed by using Attenuated Total Reflectance-Fourier Transform Infrared (ATR-FTIR). With regards to membrane performances, the tests on lateral wicking rate and protein binding ability of membrane were carried out. Membranes were tested under lateral diffusion of phenol red solution and deionised water in order to obtain the correlation between membrane pore connectivity and lateral wicking rate. In terms of protein binding ability, the membrane was evaluated by quantitative measurement of Bovine Serum Albumin (BSA) that bound onto the membrane surface.

It is essential to find the correlations and optimum casting conditions for different membrane formulations. Thus, the experimental data were further studied using the Mixture-Process Crossed Design, to analyse the influences of casting formulation, casting conditions and their interactive effects on the final membrane structure. This was followed by determination of optimum casting condition and formulation from sets of experimental data collected.

This research was continued with the modification of the membrane morphology through thermal mechanical stretching technique. A membrane stretching machine was designed for the purpose of modifying the morphologies and thus enhancing its performances. In this study, the membrane stretcher was designed based on the essential factors that influence the membrane pore structure, namely temperature, stretching speed and the extent of elongation. By using an in-house machine, the process variables such as stretching speed (0.02 to 0.12 mm/s),

temperature (25 to 75 °C) and elongation (4 to 22 %) were explored. The stretched membrane was then characterized by means of its pore size, thickness and porosity. Besides structural observation under FESEM, surface roughness of the stretched membrane was further confirmed by using the Atomic Force Microscopy (AFM). Response Surface Methodology (RSM) with Central Composite Design (CCD) was performed to study the effects of stretching parameters on membrane pore structures. A polynomial model was used to represent the significant effect of the operational conditions on selected responses.

The membrane performance on protein dot staining was further tested using the optimized membrane. Investigations on the effects of protein concentration (0 to 20 mg/ml) and volume quantity (1 to 3 μ l) immobilised on the membrane surfaces were carried out. In this report, the main interest was to determine the sensitivity of membrane towards protein immobilisation through different protein volume and concentration. The synthesized NC membranes were assembled as diagnostic test kit. Its performance as immunoassay was tested and compared with the commercial membranes.

On the last part of this research, investigation of the solute transport model was carried out. This study was confined to a model which originally developed from the Fick's Second Law. Lateral hindered diffusion coefficients of protein solution (lysozyme and BSA) in each membrane were determined. The diffusion coefficients were then correlated with the membrane pore sizes.

1.8 Organization of the thesis

This thesis consists of seven chapters. A brief introduction on membrane principle with strong emphasis on nitrocellulose membrane was outlined in Chapter 1 (Introduction). Descriptions on membrane applications in lateral flow diagnostics were also included in this chapter. This was followed by problem statements in order to provide some basis to set the research direction. Based on the defined problem statement, research objectives and scopes of the study were elucidated.

Classifications of membranes were revealed in Chapter 2 (Literature Review). Past research works on the development of NC membrane as well as the potential application in immunochromatography analysis were discussed extensively. NC membrane synthesized via dry phase inversion method, including the casting formulation and casting condition were reviewed and highlighted. The common modification methods on membrane morphology were also outlined and discussed in this chapter. The following section of the chapter included the working mechanism and conditions of immunochromatography testing.

In Chapter 3 (Membrane Diffusion Model), special attention was given on the solute transport model. It did not cover all the theories, but provided a summary of theories that were most frequently used to describe liquid diffusion. Mathematical derivation of the transport model for lateral diffusion in NC membrane was explained in details.

Chapter 4 (Materials and Method) provided details of materials and experimental procedures. These procedures included membrane preparation methods,

detailed setup and operating conditions for membrane modification, characterization techniques, performance evaluations for synthesized membranes as well as the lateral diffusion test in the membrane.

Chapter 5 (Synthesis, Characterization and Modification) and Chapter 6 (Performance Evaluation and Modeling) were the core of this thesis, which presented and discussed all the important findings based on the present experimental works. The experimental studies were carried out based on the objectives outlined in Section 1.6. In Chapter 5, the studies could be generalized as membrane fabrication, characterization, modification of membrane morphology and statistical analysis to investigate the significance of several main parameters against membrane fabrication and modification. Meanwhile, Chapter 6 focused on evaluation of membrane performances (dot staining and immunochromatography testing) and modeling of lateral hindered diffusion of protein (lysozyme and BSA) in a lateral flow membrane system.

Findings from these studies were summarized in Chapter 7 (Conclusions, Recommendations and Future Directions). Concluding remarks were given for each of the findings reported in Chapter 5 and Chapter 6, which included the membrane fabrication, membrane modification, statistical analysis, membrane performance evaluations as well as the modeling work. Based on the research findings and limitations encountered in the present works, recommendations and directions for the future research were suggested.

CHAPTER 2

LITERATURE REVIEW

2.1 Membrane classification

The most commercially utilized membrane in separation industry is made of polymeric materials. Polymeric membranes can be classified based on their surface chemistry, composition, morphology, production method or functionality. The clearest possible distinction is classification based on their nature, which is either biological or synthetic membrane (Mulder, 2003). These two types of membranes differ completely in structure and functionality. Biological membrane, with the exception of cell membrane, is thin sheets of tissues that cover various organs of human body or plant. Synthetic membrane is a artificially created membrane which is intended for separation purposes in the industries (Pinnau and Freeman, 1999).

Synthetic membranes are sub-classified by their composition, structure, and functionality. Composition refers to materials used to make the membrane, including polymers (for example cellulose nitrate, polyamide and polysulfone), ceramics, metal or carbon (Baker, 2000). Structure refers to the microstructure of the membrane in cross-section whether it is sponge type, fingerlike structure or composite. Membrane structure has proven to be an extremely illustrative route because the morphology determines the separation mechanism and hence the application. For solid synthetic membranes, three types of membrane structure may be distinguished, mainly dense membranes, asymmetric membrane and porous membranes (Wrasidlo, 1986).

Dense membrane is a thin layer of dense material utilized in the separation of small molecules. Transport through these membranes is governed not only by diffusion, but also by the solubility of the chemical species present in the membrane. Permeability depends on the thicknesses and chemical nature of the membrane (Pinto *et al.*, 1999). The structure of dense membrane can either be in a rubbery state or glassy state at a given temperature, depending on its glass transition temperature (Osada and Nakagawa, 1992).

The term asymmetric is used to refer to membrane that shows important variation in the cross-section of their structure (Pinto *et al.*, 1999). Asymmetric membrane is a composite membrane which has an active (skin) layers formed on top of the porous support. Both might be from different materials, which are selected for optimum functionality (Baker, 2000).

Porous membrane comprises of a solid matrix with pore diameters ranging from 5 nm to 50 μm . These membranes are intended for separation of larger molecules such as solid colloidal particles, for microfiltration, ultrafiltration, and dialysis applications. The structure of porous membrane is closely related to the interaction between polymer and solvent, components concentration and molecular weight in solution (Osada and Nakagawa, 1992). Thicker porous membrane sometimes provides support for the thin dense membrane layer, forming asymmetric membrane structure.

Functional classification of membranes is based on the transport phenomena, where membranes are classified according to the size of the intended separation

components, as shown in Table 2.1. For example, within porous membranes itself, a distinction is made between microfiltration (MF), ultrafiltration (UF) and reverse osmosis (RO), depending on the pore sizes and particle sizes involved (Bitter, 1991).

Table 2.1: Membrane pore size versus solutes separation in membrane processes (Cheryan, 1998)

| Size | Molecular Weight | Example | Membrane Process |
|-------------------------------|------------------|--------------------------|------------------|
| 100 μm | | Pollen | MICROFILTRATION |
| 10 μm | | Starch | |
| 1 μm | | Blood cells | |
| | | Bacteria | |
| | | Latex emulsion | |
| 1000 \AA (100 nm) | 100,000 | Albumin | ULTRAFILTRATION |
| 100 \AA | 10,000 | Pepsin | |
| | | Vitamin B-12 | |
| 10 \AA | 1000 | Glucose | NANOFILTRATION |
| | | Water | REVERSE OSMOSIS |
| | | Na^+Cl^- | |

RO retains all components other than solvent. Membrane for nanofiltration has pores larger than RO membrane but too small to allow permeation of organic compounds such as sugars. As shown in Table 2.1, ultrafiltration retains macromolecule or particle larger than about 1 nm to 50 nm. Microfiltration, on the other hand, is designed to retain particles in the micron range that is in the range of 0.1 μm to 20 μm (Cheryan, 1998). Membranes for use in microfiltration have pores

which are visible under normal light magnification, while those for use in reverse osmosis and ultrafiltration will not show any visible pores (Kesting, 1980).

2.2 Chronological development of nitrocellulose membrane

The use of naturally occurring polymer as material in microfiltration dates from antiquity. However, history of synthetic polymeric membranes began in 1855 after the invention by Fick (Cheryan, 1998). On his first synthetic membrane, he made it apparently out of cellulose nitrate to perform his diffusion studies (Kesting, 1985). In the same year, it was Lhermite who first stated that permeation occurs due to the interaction of permeate species with the membrane. By varying the polymer concentration, Bechhold had prepared a series of microfiltration membranes with graded pore size in 1907. He is also the first to develop a method to measure the pore diameters by using air pressure and surface tension measurements (Cheryan, 1998).

Until 1945, membranes with micron size were used primarily for diffusion studies, sizing of macromolecules and removal of microorganisms and particles from liquid (Cheryan, 1998). Since then, several major commercial developments in membrane science had taken place. However, before 1960, there was no significant membrane industry existed, probably due to the expensive cost, slow and unselective membrane performances (Baker, 2000). In 1960, Loeb and Sourirajan succeeded in developing a method of manufacturing asymmetric membrane. The obtained membrane had high permeability and led to the widest possible range of applications (Cheryan, 1998).

In 1963, it was first reported that nitrocellulose (NC) membrane has a strong adsorption on single stranded DNA (Nygaard and Hall, 1963). This NC membrane was later developed for blotting protein fractions from sodium dodecyl sulfate polyacrylamide gel electrophoresis (SDS-PAGE) and this process is made known as “Western Blotting”. At present, lateral flow NC membrane with high mechanical stability and tensile strength constitutes as important element for rapid diagnostic test strips (Mahendran *et al.*, 2005). NC membrane has shown to be a common and convenient carrier material in small scale chromatography or protein electrophoresis manufacturing.

Significant progresses have been made in virtually every phase of membrane developments in membrane applications, formation processes, chemical structures and physical structures. Although the basic principles and methodologies have already been established, the tailor making and optimization of the membrane for specific applications had just begun. Over the past 40 years, solutions after solutions for these problems have been developed, making membrane-based separation process become one of the most common processes in separation industries. As we welcome ourselves into the 21st century, new development of membrane technology for immunodiagnostic will further widen the applicability of membrane in biomedical sector.

2.3 Properties of NC membrane

Chemistry of synthetic membrane refers to the chemical nature and composition of the membrane surface that is used in a separation process (Zeman and Zydney, 1996). The membrane surface chemistry creates important properties such

as hydrophilicity or hydrophobicity (relates to the surface free energy), ionic charges, chemical or thermal resistance, binding affinity for particles in a solution, and biocompatibility (in the case of bio-separation) (Zeman and Zydney, 1996). The membrane properties can be very different from its bulk composition, whereby polymer contributes specifically to physical or chemical nature of the membrane.

2.3.1 Chemical and physical properties of NC polymer

Nitrocellulose (NC) or cellulose nitrate polymer known as Type “RS” or Type “E” (11.8-12.3% N) is one of the famous polymers used in producing lateral flow membrane with high porosity, high pore connectivity and high binding affinity. NC is the first synthetic polymer and also the first polymer utilized in the preparation of a synthetic membrane in 1855 (Kesting, 1985). Its highly hydrophobic glassy polymer consists of cellulose that is nitrating by three nitrate groups per glucose molecule, as shown in Figure 2.1.

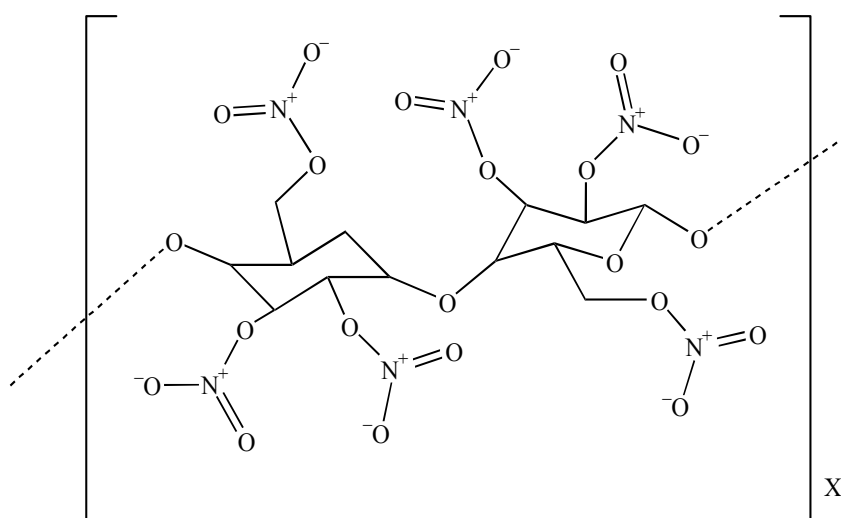
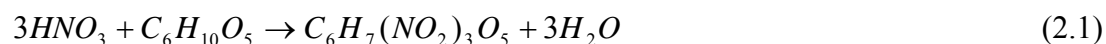


Figure 2.1: Chemical structure of nitrocellulose polymer

NC polymer is made by first order reaction of the cellulose through the exposure to nitric acid, as shown in Equation 2.1. The produced polymer is highly flammable and needs to be stored in wet condition to avoid explosion.



In terms of the polymer chemistry, NC is categorised as Lewis acid and soluble in a wide range of low cost organic solvents such as acetone and methyl acetate (Kesting, 1985). It is utilized in substantial quantities in the production of microfiltration membranes either by itself or in conjunction with other cellulosic polymers, with the addition of solvents. Once widely utilized together with camphor as a general plastic known as celluloid, NC has surrendered most of these applications to cheaper and less flammable materials. Nevertheless, its toughness, adhesive nature, and transparency has permitted it to remain competitive and survived as an item of commerce today (Mehta and Rajput, 1998).

2.3.2 Structural and characterization of NC membrane

The range of pores of NC membrane that can be manufactured is from 0.05 to about 12 μm , where this range of pores is very suitable for use in microfiltration (Kesting, 1985). In term of mechanical strength, NC membrane is more friable compared to analogous membranes from nylon, polysulfone, or certain acrylic co-polymers (Ben Rejeb *et al.*, 1998). Nevertheless, the membrane is quite resistant to chlorinated hydrocarbons which are solvents or swelling agents for polymers including polysulfone, polycarbonate, and polyvinylidene fluoride (Kesting, 1985).

Compared to other cellulosic membrane, such as cellulose acetate or cellulose triacetate membrane, NC membrane is more resistive to shrinkage during autoclaving.

Different membrane forming materials have intrinsic affinity binding capacity for different proteins. One of the special features of NC membrane is the high binding capacity and large void volume between the membrane pores. This feature offers good accessibility and large surface area for potential adsorption of protein molecules. A pure NC membrane has optimal protein binding capacity in the range of 80 to 100 $\mu\text{g}/\text{cm}^2$ (Kung, 1991). Thus, most of the membrane applications are based on the analytical protein blotting protocols, including protein immobilization, protein binding assays and lateral-flow immunochromatographic testing (Graf and Friedl, 1999; Beer *et al.*, 2002; Czerwinski *et al.*, 2005). NC membrane assures the required membrane sensitivity level applied in an immunoassay. A NC membrane is capable to bind 50-80 $\mu\text{g}/\text{cm}^2$ of single-stranded DNA while cellulose acetate membrane only binds 1 $\mu\text{g}/\text{cm}^2$ (Oey and Knippers, 1972).

Liquid migration speed which depends on the membrane diffusion resistant is another important feature of NC membrane (Oey and Knippers, 1972). Technically speaking, liquid migration trend reflects the surface properties and porosity of the membrane, and probably be used in the membrane homogeneity measurement. The distribution of the liquid solution in the membrane strip can occur in two ways, either perpendicularly through the membrane or through slip flow on one side of the membrane strip (lateral flow liquid distribution) (Konopka *et al.*, 2002). Wicking test is used to determine the liquid migration speed at which a liquid sample moves along

the membrane strip. An easier parameter to measure the liquid flow rate is the capillary flow time (s/cm), which is defined as the time required for liquid to move along and fill completely the membrane strip of defined length.

2.4 Potential application of NC membrane in immunoassay

Membrane separation process has experienced a remarkable growth in the biomedical industry. In recent years, lateral flow immunochromatographic assays have been widely introduced in the field of biomedical and healthcare analysis, due to their high sensitivity and specificity, rapid testing, inexpensive manufacturing cost and user-friendly operating procedure (Newman and Price, 1997; Hampl *et al.*, 2001; Czerwinski *et al.*, 2005; Wang *et al.*, 2006). A large number of tests are available for the detection of infectious diseases (Schramm *et al.*, 1998; Zhang *et al.*, 2006), food hygiene (Bird *et al.*, 1999; Hatta *et al.*, 2002; Aziah *et al.*, 2007), fertility test and etc. Use of these kits will translate to the swift detection of fatal diseases, which will help to save lives.

Membrane is probably the single most important material used in lateral flow immunodiagnostic strip. The choice of a membrane largely depends on the protein-binding capacity, porosity and lateral wicking speed of the membrane. Among the membranes, lateral flow NC membrane is known as the most popular transport medium in an immunoassay (Lonnberg and Carlsson, 2001; Qian and Bau, 2004). The flow-through biosensors based on protein or DNA micro-arrays make use of thin porous nitrocellulose membrane, where such micro-array methods can detect specific interactions between the analyte and the spotted capture probes including DNA hybridisation, disease diagnosis and genome research (Kurt *et al.*, 2008).

NC membrane has long occupied a position of central importance in medical and immunological analysis due to its excellent wetting properties, high binding capacity and low background staining (Morais *et al.*, 1999; Sun *et al.*, 2008). The membrane has been widely used in a vast fields of study, such as protein research (Lonnberg and Carlsson, 2001; Czerwinski *et al.*, 2005), lateral flow immunochromatography testing (Mahendran *et al.*, 2005), protein immobilization (Bialopiotrowicz and Janczuk, 2002) and western blotting (Oehler *et al.*, 1999). The used of NC membrane made possible the development of immunoassay based on the interaction between antibodies and antigens, as well as the refinement of immunodiagnostic into lateral-flow, point-of-care assays (Beer *et al.*, 2002; Oh *et al.*, 2009).

2.5 Development of NC membrane

Studies of the membrane surface and internal layers are fundamental in the development of lateral flow membrane as one of the processing materials in medicine and health care analysis devices. If the membrane structures can be controlled precisely, various kinds of immunological analysis can be performed effectively and accurately.

Porosity and pore size are the key factors to determine the membrane quality and performance. Membrane with smaller pores or lower porosity would exhibit higher resistance in lateral flow rate, and thus converting to a longer liquid wicking time. Contrary, bigger membrane pore or higher porosity contributes to a faster liquid wicking time but at the expense of membrane protein-binding ability. Besides,

the mechanical properties can be adversely affected if the membrane pore is too large and if there is incomplete connection between the polymer particles (Kesting, 1985).

Membrane production is, nonetheless, a very sensitive process. Several strategies are cited in order to control the membrane morphologies, including the fabrication techniques, formulations and preparation conditions (Lin *et al.*, 1998; Chan and Tsao, 2003). The mechanism of membrane formation was said to be rather complex as there are various fabrication factors need to be considered during the casting stage, and its final performance is strongly dependent on those fabrication factors. In membrane formulation, factors that need to be taken into account are the choices of casting materials, composition of casting solution and gelation-crystallization behaviour of the polymer (Pinnau and Koros, 1993; Vaessen *et al.*, 2002). At the same time, parameters of the casting process such as relative humidity, casting speed, casting thickness, evaporation time and drying temperature also need to be considered simultaneously. By manipulating the initial phase transition and rheological factors, the porous membranes can be prepared at desired pore size, porosity, thickness, and surface roughness (Mulder, 2003; Meier *et al.*, 2004; Khayet *et al.*, 2005).

2.5.1 Membrane fabrication technique: Phase inversion

Numerous methods are known for generating the thin film membrane with micron-scale closed pores or opened pores structures. These include sintering, stretching, track-etching, sol-gel process, vapour deposition, solution coating and phase inversion, as shown in Table 2.2 (Kesting, 1985; Cheryan, 1998; Mulder, 2003). Each of these methods results in different membrane morphology, porosity